Dark photon dark matter from an oscillating dilaton

Peter Adshead,[1,2,*] Kaloian D. Lozanov,[1,3,†] and Zachary J. Weiner[4,‡]

[1]*Illinois Center for Advanced Studies of the Universe and Department of Physics, University of Illinois at Urbana-Champaign, Urbana, Illinois 61801, USA*

[2]*Center for Particle Cosmology, Department of Physics and Astronomy, University of Pennsylvania, 209 South 33rd St, Philadelphia, Pennsylvania 19104*

[3]*Kavli IPMU (WPI), UTIAS, The University of Tokyo, 5-1-5 Kashiwanoha, Kashiwa, Chiba 277-8583, Japan*

[4]*Department of Physics, University of Washington, Seattle, Washington 98195, USA*

(Received 3 February 2023; accepted 1 April 2023; published 19 April 2023)

We present a mechanism for generating ultralight dark photon dark matter in the early Universe via a dilatonlike scalar field coupled to the dark photon's kinetic term. Energy is initially stored in the condensate of the dilaton, which resonantly produces dark photons when it begins oscillating in the early Universe. While similar scenarios with axion–dark-photon couplings require large coupling coefficients to fully populate the dark photon, the dilatonic coupling features a unique regime: When the dark photon's mass is half that of the dilaton, dark photons are copiously produced even when the dilaton undergoes small-amplitude oscillations. Scenarios consistent with the cosmic microwave background allow for ultralight vector dark matter with mass as light as 10^{-20} eV.

DOI: 10.1103/PhysRevD.107.083519

I. INTRODUCTION

Ultralight, massive dark photons (i.e., spin-1 vector bosons) are a curious candidate for the dark matter (DM) in our Universe. Like scalar fuzzy DM [1–4], ultralight dark photons exhibit wavelike properties on macroscopic scales, $\lambda \lesssim 10$ pc, for masses $m_{\gamma'} \gtrsim 10^{-21}$ eV [5,6]. Halos supported by dark photons can therefore feature vector solitonic cores [5] reminiscent of those in scalar fuzzy DM models [1]. However, these vector solitons are distinguished due to their intrinsic spins [7,8]. The vectorlike nature of the condensate also allows for distinctive higher energy solitonic configurations similar to Proca stars with radially directed vector fields [5]. Furthermore, stable starlike solutions are possible when self-interactions of the dark photons are included [9,10]. Vector dark matter's predictions for small-scale structure also differ considerably from its scalar cousin due to the nature of its production mechanisms, which typically result in a highly peaked power spectrum on small scales [11–15]. Such a peaked spectrum leads to rich small-scale structure, with significant energy density stored in boson stars [8,16].

Recent studies on dynamical heating of ultrafaint dwarf galaxies via coherent fluctuations in fuzzy dark matter put pressure on the very low mass end of the mass spectrum, requiring $m_{\rm fdm} > 10^{-19}$ eV [17]. Slightly weaker limits are expected to apply to the vector scenario due to the reduced interference of the multiple polarization states [8]. Reference [18] argues that a generic bound $m_{\rm fdm} > 10^{-18}$ eV applies when dark matter is produced by a causal process after inflation. While scalar [19–22] and vector [23,24] masses in the range 10^{-13}–10^{-11} eV are constrained by solar-mass black hole superradiance bounds (and lighter masses could be probed by supermassive black holes [22]), these can be evaded by self-interactions of the vector field [15], leaving a wide range of masses viable.

Production of dark photon DM in the ultralight particle mass range is a longstanding problem. Early models that produced dark photons from a misalignment mechanism analogous to that of scalar dark matter production [25] were later shown to require nonminimal couplings to the Ricci scalar [26–28] that can lead to violations of unitarity at relatively low energy scales in longitudinal graviton-photon scattering [15]. Massive dark photons minimally coupled to Einstein gravity (but otherwise decoupled from other matter fields) are produced during slow-roll inflation, but their abundance matches the one of DM only if $m_{\gamma'} \gtrsim 10^{-5}$ eV [11,29–31]. Finally, an oscillating Higgs [32] or an oscillating, misaligned axion [15,33]

*adshead@illinois.edu
†kaloian.lozanov@ipmu.jp
‡zweiner@uw.edu

allow for the resonant production of ultralight dark photons with the correct DM abundance. While these resonant vector DM production models are based on well-motivated theories, they pose questions about naturalness and choices of couplings. In particular, the dimensionless coupling constants should respect a hierarchy in the case of the oscillating Higgs [32], and in the axion models, large couplings between the axion and the Chern-Simons term, $F\tilde{F}$, of the vector field are exacerbated by the small gauge couplings that are required [15,33].

In this work, we identify a new variant of the resonant mechanism for generating dark photon DM that does not require unnaturally large couplings. In addition to the dark photon, we consider a scalar (or "dilaton") ϕ kinetically coupled to the dark photon via an interaction $\mathcal{L} \supset W(\phi)F_{\mu\nu}F^{\mu\nu}/4$. This form of interaction was studied in Refs. [34,35], where ϕ played the role of the inflaton. During slow-roll inflation, ultralight dark photons can be produced with the right DM abundance provided that the effective dependence of the coupling on the Friedmann-Lemaître-Robertson-Walker (FLRW) scale factor is $W(\phi(a)) \propto a^{-n}$ for n close to 4. Reference [36] considered a spectator ϕ whose evolution during inflation produces large-wavelength dark photons. In this work, we instead consider ϕ to be a light spectator field during inflation whose postinflationary oscillations (rather than its inflationary dynamics) give rise to the resonant production of vector DM.

When the dilaton oscillates with large amplitude [$\phi/M \gg 1$, where M is the mass scale associated with the coupling function $W(\phi)$], dark photons are efficiently produced via broad resonance, closely resembling models that feature a coupling to an axion [15,33]. Typically, such parametric resonances become inefficient for small oscillation amplitudes $\phi/M < 1$, below which

$$W(\phi) \approx 1 + \phi/M + \mathcal{O}[(\phi/M)^2]. \tag{1}$$

As such, large couplings are required to completely deplete the dilaton (or axion) condensate into the vector. However, the dilatonic coupling exhibits a unique regime. When the vector mass is half the dilaton mass, $m_{\gamma'} = m_\phi/2$, a low-momentum instability becomes efficient at late times, i.e., under *small* amplitude oscillations $\phi < M$. We show this explicitly for the benchmark model $W(\phi) = e^{\phi/M}$, but our main results depend only on the small-amplitude behavior being of the form Eq. (1). With $M \approx 10^{17}$ GeV, the model successfully realizes ultralight vector DM scenarios ($m_{\gamma'} \sim 10^{-21}$ eV) consistent with cosmic microwave background (CMB) bounds on isocurvature perturbations and the scale of inflation. Unlike existing resonance mechanisms [15,33], this mechanism therefore does not require a large coupling between the dark photon and the scalar, instead requiring a specific tuning between the masses of the scalar and dark photon.

In the remainder of this paper, we detail the governing equations for a massive vector coupled to a dilaton (Sec. II), study the resonant production of dark photons due to an oscillating dilaton (Sec. III), and present the resulting relic abundance of dark photon dark matter and viable parameter space given various cosmological constraints (Sec. IV). We conclude in Sect. V. Throughout, we work with an FLRW metric of the form

$$\mathrm{d}s^2 = -\mathrm{d}t^2 + a(t)^2\delta_{ij}\mathrm{d}x^i\mathrm{d}x^j, \tag{2}$$

with $a(t)$ the scale factor. We use natural units in which $\hbar = c = 1$ and the reduced Planck mass $m_{\rm Pl} = 1/\sqrt{8\pi G}$. Greek spacetime indices are contracted via the Einstein summation convention, while repeated Latin spatial indices are contracted with the Kronecker delta function (regardless of their placement). Dots denote derivatives with respect to cosmic time t, and the Hubble rate is $H \equiv \dot{a}/a$.

II. MODEL AND DYNAMICS

We consider a dilatonlike scalar ϕ coupled to a vector A_μ via the action

$$S = \int \mathrm{d}^4x\sqrt{-g}\left[\frac{m_{\rm Pl}^2}{2}R - \frac{1}{2}\partial_\mu\phi\partial^\mu\phi - \frac{1}{2}m_\phi^2\phi^2 - \frac{W(\phi)}{4}F_{\mu\nu}F^{\mu\nu} - \frac{1}{2}m_{\gamma'}^2A_\mu A^\mu\right], \tag{3}$$

where $F_{\mu\nu} = \partial_\mu A_\nu - \partial_\nu A_\mu$ and R is the Ricci scalar. The modulation of the dark photon kinetic term by $W(\phi)$ can be interpreted as a ϕ dependence of the dark $U(1)$ coupling strength. The dark photon mass term could arise through the Stueckelberg or Higgs mechanisms. In general, $m_{\gamma'}$ could be a function of ϕ, but its ϕ dependence need not coincide with the one of the dark photon gauge coupling. For simplicity, throughout this work, we treat $m_{\gamma'}$ as a constant Stueckelberg/Proca mass term.

The Euler-Lagrange equations for Eq. (3) are

$$0 = -\nabla_\mu\nabla^\mu\phi + m_\phi^2\phi + \frac{W'(\phi)}{4}F_{\mu\nu}F^{\mu\nu} \tag{4a}$$

$$0 = -\nabla_\mu[W(\phi)F^{\mu\nu}] + m_{\gamma'}^2A^\nu. \tag{4b}$$

Equation (4b) implies that

$$\nabla_\mu A^\mu = 0, \tag{5}$$

which coincides with the Lorenz gauge choice (for gauge theories) but is instead here a constraint imposed by consistency of the equations of motion. In FLRW spacetime, Eq. (2) and Eqs. (4a) and (4b) reduce to

$$0 = \ddot{\phi} + 3H\dot{\phi} - \frac{1}{a^2}\partial_i\partial_i\phi + m_\phi^2\phi + \frac{W'(\phi)}{4}F_{\mu\nu}F^{\mu\nu} \tag{6a}$$

$$0 = \ddot{A}_0 + 3H\dot{A}_0 + 3\dot{H}A_0 - \frac{1}{a^2}\partial_j\partial_j A_0 + \frac{2H}{a^2}\partial_i A_i + \frac{m_{\gamma'}^2}{W(\phi)}A_0 - \frac{1}{a^2}\frac{\partial_i W(\phi)}{W(\phi)}(\partial_i A_0 - \dot{A}_i) \tag{6b}$$

$$0 = \ddot{A}_i + H\dot{A}_i - \frac{1}{a^2}\partial_j\partial_j A_i + 2H\partial_i A_0 + \frac{m_{\gamma'}^2}{W(\phi)}A_i - \frac{\partial^\mu W(\phi)}{W(\phi)}F_{\mu i}. \tag{6c}$$

We expand the vector in Fourier modes as

$$A_0(t,\mathbf{x}) = \int \frac{\mathrm{d}^3k}{(2\pi)^3}e^{i\mathbf{k}\cdot\mathbf{x}}A_0(t,\mathbf{k}) \tag{7}$$

$$A_j(t,\mathbf{x}) = \sum_{\lambda\in\{\pm,\|\}}\int \frac{\mathrm{d}^3k}{(2\pi)^3}e^{i\mathbf{k}\cdot\mathbf{x}}A_\lambda(t,\mathbf{k})\epsilon_j^\lambda(\mathbf{k}), \tag{8}$$

where the polarization vectors satisfy

$$\begin{aligned} \epsilon_m^\lambda(\mathbf{k})^*\epsilon_m^{\lambda'}(\mathbf{k}) &= \delta^{\lambda\lambda'} \qquad ik_m\epsilon_m^\pm(\mathbf{k}) = 0 \\ \epsilon_m^\lambda(\mathbf{k}) &= \epsilon_m^\lambda(-\mathbf{k})^* \qquad ik_m\epsilon_m^\|(\mathbf{k}) = k \\ i\varepsilon_{lmn}k_m\epsilon_n^\pm(\mathbf{k}) &= \pm\epsilon_l^\pm(\mathbf{k}) \qquad i\varepsilon_{lmn}k_m\epsilon_n^\|(\mathbf{k}) = 0, \end{aligned} \tag{9}$$

and we likewise expand the dilaton into

$$\phi(t,\mathbf{x}) = \bar{\phi}(t) + \int \frac{\mathrm{d}^3k}{(2\pi)^3}e^{i\mathbf{k}\cdot\mathbf{x}}\delta\phi(t,\mathbf{k}). \tag{10}$$

To linear order in spatial fluctuations, Eq. (6c) then decomposes into

$$0 = \ddot{A}_\pm + \left(H + \frac{\dot{\bar{W}}}{\bar{W}}\right)\dot{A}_\pm + \left(\frac{k^2}{a^2} + \frac{m_{\gamma'}^2}{\bar{W}}\right)A_\pm \tag{11a}$$

$$0 = \ddot{A}_\| + \left(H + \frac{\dot{\bar{W}}}{\bar{W}}\right)\dot{A}_\| + \left(\frac{k^2}{a^2} + \frac{m_{\gamma'}^2}{\bar{W}}\right)A_\| + \left(\frac{\dot{\bar{W}}}{\bar{W}} - 2H\right)kA_0, \tag{11b}$$

using the shorthand $\bar{W} = W(\bar{\phi})$. The Lorenz constraint Eq. (5) sets

$$kA_\|/a^2 = \dot{A}_0 + 3HA_0, \tag{12}$$

which combines with Eq. (6b) to give

$$0 = \ddot{A}_0 + 5H\dot{A}_0 + \left(\frac{k^2}{a^2} + \frac{m_{\gamma'}^2}{\bar{W}} + 3\dot{H} + 6H^2\right)A_0. \tag{13}$$

Note that the third-order differential equation yielded by substituting Eq. (12) for $A_\|$ in Eq. (11b) is proportional to the time derivative of Eq. (13) plus $3H + \dot{\bar{W}}/\bar{W}$ times Eq. (13); i.e., the system is self-consistent.

The dynamics of the transverse modes and A_0 are most conveniently studied in terms of the rescaled fields

$$\mathcal{A}_\pm \equiv \sqrt{a\bar{W}}A_\pm \tag{14a}$$

$$\mathcal{A}_0 \equiv a^{5/2}A_0, \tag{14b}$$

for which Eqs. (11a) and (13) respectively reduce to

$$\ddot{\mathcal{A}}_\pm = -\left[\frac{k^2}{a^2} + \frac{m_{\gamma'}^2}{\bar{W}} - \frac{\partial_t^2\sqrt{\bar{W}}}{\sqrt{\bar{W}}} - \frac{H\dot{\bar{W}}}{2\bar{W}} - \frac{\dot{H}}{2} - \frac{H^2}{4}\right]\mathcal{A}_\pm \tag{15a}$$

$$\ddot{\mathcal{A}}_0 = -\left(\frac{k^2}{a^2} + \frac{m_{\gamma'}^2}{\bar{W}} + \frac{\dot{H}}{2} - \frac{H^2}{4}\right)\mathcal{A}_0. \tag{15b}$$

In general, $W(\phi) \to 1$ at late times (as ϕ decays with expansion), and $\mathcal{A}_\pm$ and $\sqrt{a}A_\pm$ then coincide, but an instability analysis is more straightforward in terms of the former. In addition, Eq. (12) sets

$$A_\| = \frac{1}{\sqrt{a}k}\left(\dot{\mathcal{A}}_0 + \frac{H}{2}\mathcal{A}_0\right); \tag{16}$$

i.e., one can study the (relatively simpler) dynamics of Eq. (15b) in place of the longitudinal mode.

III. STABILITY ANALYSIS

To characterize the (in)stability of vector modes in an oscillating dilaton background, we first consider the limiting case of Minkowski spacetime. We then apply these results to FLRW spacetime, relying on the fact that (for the parameter space of interest) the relevant dynamics occur on timescales much shorter than the instantaneous Hubble rate.

A. Small-amplitude broad resonance in Minkowski spacetime

In Minkowski (i.e., nonexpanding) spacetime, the homogeneous component of the dilaton evolves according to

$$\ddot{\bar{\phi}} + m_\phi^2\bar{\phi} = 0, \tag{17}$$

solved by $\bar{\phi}(t) = \phi_0\cos(m_\phi t)$ under the initial condition $\bar{\phi}(t) \to \phi_0$ and $\dot{\bar{\phi}}(t) \to 0$ for $t \ll 1/m_\phi$. For concreteness, we set

$$W(\phi) = e^{\phi/M}, \tag{18}$$

for which Eqs. (15a) and (15b) (after substituting $a = 1$ and $H = 0$) are

$$\ddot{\mathcal{A}}_\pm = -\left[k^2 + \frac{m_{\gamma'}^2}{e^{\bar{\phi}/M}} - \frac{\ddot{\bar{\phi}}}{2M} - \left(\frac{\dot{\bar{\phi}}}{2M}\right)^2\right]\mathcal{A}_\pm \tag{19a}$$

$$\ddot{\mathcal{A}}_0 = -\left(k^2 + \frac{m_{\gamma'}^2}{e^{\bar{\phi}/M}}\right)\mathcal{A}_0. \tag{19b}$$

Because $\bar{\phi}(t)$ is periodic, Eqs. (19a) and (19b) describe harmonic oscillators with periodic frequencies. By the Floquet theorem [37,38], their solutions are of the form $\mathcal{P}_+(t)e^{\mu t} + \mathcal{P}_-(t)e^{-\mu t}$, where μ is the Floquet exponent and $\mathcal{P}_\pm(t) = \mathcal{P}_\pm(t+T)$, with T being the period of the background. Modes for which $\Re(\mu) \neq 0$ are unstable and grow exponentially with time. We next study the structure of parametric instabilities in these equations.

For massless dark photons, unstable solutions are present only for sizeable oscillation amplitudes, $\phi_0 \gtrsim M$. While massive dark photons also experience these large-amplitude instabilities (provided the mass is not too large, i.e., $m_{\gamma'} \lesssim \dot{\bar{W}}/\bar{W} \sim m_\phi$), the presence of the mass term gives rise to a novel low-momentum ($k \ll m_\phi$) instability in the small-amplitude ($\phi_0 \ll M$) regime when $m_{\gamma'}/m_\phi = 1/2$. To see how this instability arises, we first note that in this limit and to leading order in ϕ_0/M, Eqs. (19a) and (19b) tend to the Mathieu equation

$$0 = \frac{\mathrm{d}^2 X}{\mathrm{d}z^2} + [p - 2q\cos(2z)]X(z), \tag{20}$$

where

$$z = \frac{m_\phi t}{2} \tag{21a}$$

$$p = \left(\frac{2k}{m_\phi}\right)^2 + \left(\frac{2m_{\gamma'}}{m_\phi}\right)^2 \tag{21b}$$

$$q = \frac{2\phi_0}{M}\frac{m_{\gamma'}^2}{m_\phi^2} \times \begin{cases} 1 & X = \mathcal{A}_0 \\ 1 - m_\phi^2/(2m_{\gamma'}^2) & X = \mathcal{A}_\pm. \end{cases} \tag{21c}$$

The solution to the Mathieu equation [37], $\tilde{\mathcal{P}}_+(t)e^{\tilde{\mu}z} + \tilde{\mathcal{P}}_-(z)e^{-\tilde{\mu}z}$, is unstable for small q provided that $p = n^2$ for integer n. For instance, the case $n = 1$, corresponding to $m_{\gamma'} = m_\phi/2$ for modes $k \ll m_\phi$, gives rise to an unstable solution in the limit of small q (and therefore of small amplitude). The Floquet exponent of the Mathieu equation in this regime is known analytically to be $\lim_{q\to 0}\Re(\tilde{\mu}^{n=1}) \approx |q|/2$ [37], yielding[1]

$$\Re(\mu) \approx \frac{m_\phi}{8}\frac{\phi_0}{M} \tag{22}$$

for the solutions to Eqs. (19a) and (19b) when $\phi_0 \ll M$ and $k \ll m_\phi$.

Figure 1 depicts the Floquet exponents for the transverse [Eq. (19a)] and longitudinal [Eq. (19b)] components as a function of the vector's wave number and the dilaton's oscillation amplitude. In addition to the broad instability bands for large momenta and amplitudes, Fig. 1 exhibits the above-described band at small k/m_ϕ extending down to $\phi_0/M \to 0$. We note that the unstable band does not extend to arbitrarily small amplitudes if $m_{\gamma'}$ is not precisely equal to $m_\phi/2$. In particular, the width of the instability band in k in the small-q limit is $|p_{n=1} - 1| = |q|$ [37]. Quantifying the mass tuning as

$$\delta \equiv \left(\frac{m_{\gamma'}}{m_\phi}\right)^2 - \frac{1}{4}, \tag{23}$$

the width of the instability band is

$$\left|\left(\frac{k}{m_\phi}\right)^2 + \delta\right| \lesssim \frac{\phi_0}{8M}. \tag{24}$$

The low-momentum instability band vanishes for $\phi_0/M < 8\delta$ (though if $\delta < 0$, a narrow instability band persists to arbitrarily small ϕ_0/M over wave numbers satisfying $|\delta| - \phi_0/8M \lesssim (k/m_\phi)^2 \lesssim |\delta| + \phi_0/8M$). Below we estimate the level of mass tuning this implies for viable dark photon dark matter scenarios.

B. Parametric resonance in FLRW

The above results for the resonant instabilities in Minkowski spacetime can be extended to the expanding Universe by accounting for the redshifting of physical momenta k/a and of the dilaton's oscillation amplitude. Specifically, in an FLRW spacetime, the dilaton begins to oscillate when $H(t_i) \approx m_\phi$ with an initial amplitude $\phi_{0,i}$ that subsequently redshifts as[2]

$$\phi_0(t) \approx 1.5\phi_{0,i}\left(\frac{a(t)}{a_i}\right)^{-3/2} \tag{25}$$

in the radiation-dominated era. The corresponding time dependence of the coefficients in the equations of motion Eqs. (19a) and (19b), which nominally brings them away from the form of the Mathieu equation Eq. (20), is negligible when the dilaton's oscillation rate is much faster

[1]Note that for $n = 1$, the Mathieu resonance parameters q [Eq. (21c)] for $\mathcal{A}_\pm$ and $\mathcal{A}_0$ have opposite signs but the same magnitude (and therefore the same Floquet exponent).

[2]More precisely, the solution to Eq. (6a) for the homogeneous mode $\bar{\phi}(t)$ in a radiation background is $\Gamma(5/4)\phi_{0,i}J_{1/4}(m_\phi t)/\sqrt[4]{m_\phi t/2}$, where J_ν is the order-ν Bessel function. The asymptotic oscillation amplitude is $2^{3/2}\Gamma(5/4)\phi_{0,i}/(a/a_i)^{3/2}\sqrt{\pi}$.

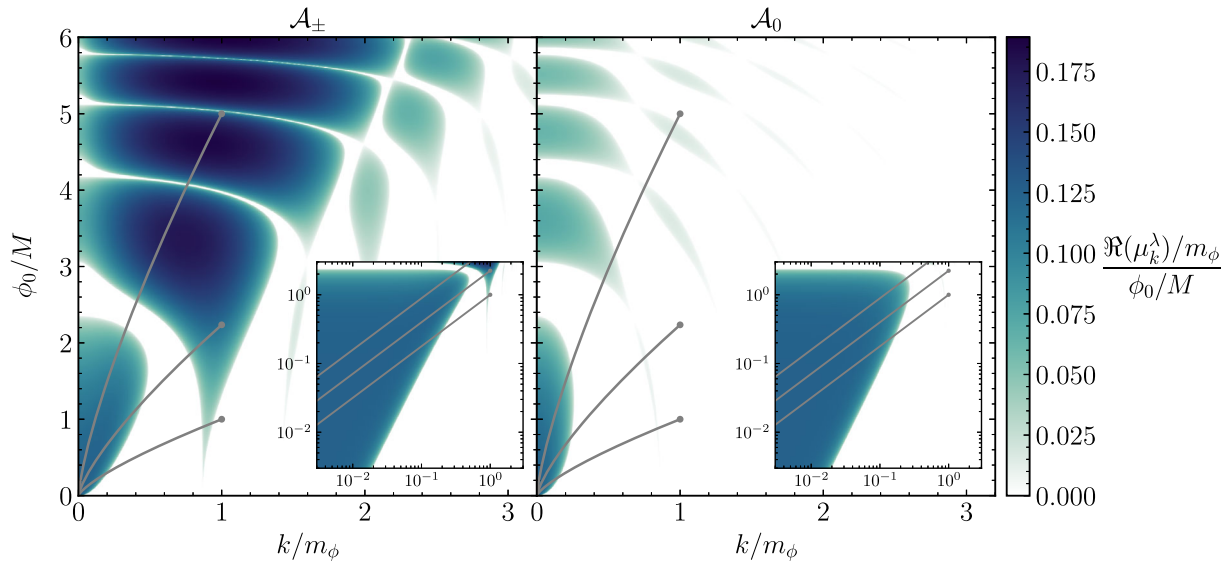

FIG. 1. Real part of the Floquet exponent μ_k for the solutions of the equations of motion describing the transverse [Eq. (19a)] and longitudinal [Eq. (19b)] sectors. Both panels fix $m_\phi = 2m_{\gamma'}$, for which a region with $\Re(\mu_k) > 0$ extends to arbitrarily small ϕ_0/M and k/m_ϕ (depicted in the inset panels). Results are scaled by ϕ_0/M to facilitate interpreting results in FLRW spacetime (see the main text for details). Note that the horizontal axis corresponds to the *physical* wave number k/a in FLRW spacetime. Gray lines depict the trajectory of the physical horizon $H(t) = m_\phi/[a(t)/a_i]^2$ for three different initial amplitudes $\phi_{0,i} = M$, $\sqrt{5}M$, and $5M$, roughly indicating the low–wave-number cutoff for resonance in the radiation era as a function of time.

than the expansion rate (which, in the radiation-dominated era, evolves as $H \propto 1/a^2$). [Likewise, the terms proportional to the Hubble rate in Eqs. (15a) and (15b) are also negligible in this limit.] That is, at sufficiently late times, the dilaton's oscillation amplitude and each mode's physical wave number are effectively constant over each oscillation. The Minkowski-space Floquet exponent Eq. (22) therefore captures the instantaneous growth rate in FLRW spacetime to good approximation upon replacing the constant ϕ_0 with the (slowly) decaying amplitude Eq. (25).

Depleting the dilaton's energy (so that the majority of the dark matter comprises dark photons) requires parametric resonance to be efficient [38], i.e., that the exponential growth rate is significantly greater than the Hubble rate ($\Re(\mu)/H \gg 1$) for a sufficiently long duration. Crucially, the expansion rate decays faster with expansion than the dilaton's oscillation amplitude [Eq. (25)] in the radiation-dominated era—namely, the exponential growth rate Eq. (22) relative to the expansion rate is

$$\frac{\Re[\mu(t)]}{H} = \frac{1}{8}\frac{3\phi_{0,i}}{2M}\left(\frac{a(t)}{a_i}\right)^{1/2}. \tag{26}$$

Hence, the efficiency (i.e., per e-fold of expansion) of resonance grows with the expansion of the Universe. Accordingly, $\Re[\mu(t)]/H$ is approximately equal to the quantity plotted in Fig. 1 times $\sqrt{a(t)/a_i}\cdot 3\phi_{0,i}/2M$. Furthermore, the comoving width of the instability band also grows with time, bounded above by $(k/m_\phi)^2 \leq \phi_{0,i}/8M \cdot (a/a_i)^{1/2}$ [via Eq. (24)] and below by the comoving horizon scale $m_\phi/(a/a_i)$ (corresponding to the gray lines in Fig. 1).

Eq. (26) shows that, even if the initial oscillation amplitude is small, after the Universe expands by a factor $\propto(\phi_{0,i}/M)^{-2}$, the rate of particle production becomes efficient. More precisely, production of the vector completes soon after its energy density becomes comparable to the dilaton's. Via Eq. (25), $\rho_\phi \approx m_\phi^2\phi_{0,i}^2/(a/a_i)^3$. Since the vector is produced well after a_i with a comoving wave number of order m_ϕ, it is nonrelativistic at production; its energy density is then approximately

$$\rho_A(t) \approx \frac{m_{\gamma'}^2}{2(a/a_i)^3\bar{W}}\sum_\lambda \langle \mathcal{A}_\lambda(t,\mathbf{x})^2\rangle, \tag{27}$$

where

$$\langle \mathcal{A}_\lambda(t,\mathbf{x})^2\rangle = \int \mathrm{d}\ln k \frac{k^3}{2\pi^2}\langle|\mathcal{A}_\lambda(t_i,k)|^2\rangle e^{2\int_{t_i}^t \mathrm{d}t'\,\Re[\mu(t)]}. \tag{28}$$

Before production, $\mathcal{A}_\lambda$ is in the vacuum state [39,40],

$$\langle|\mathcal{A}_\lambda(t_i,k)|^2\rangle = \frac{1}{2\sqrt{(k/a)^2 + m_{\gamma'}^2}}. \tag{29}$$

Setting the growth rate to that from Eq. (26) in Eq. (27), taking the integral over wave number to be dominated by modes with $k \sim m_\phi$, and noting that $\bar{W} \approx 1$ at late times,

$$\rho_A(t) \approx \frac{m_{\gamma'}^2 m_\phi^2}{(a/a_i)^3} \exp\left[\frac{3\phi_{0,i}}{4M}\left(\frac{a}{a_i}\right)^{1/2}\right]. \tag{30}$$

The dilaton and vector have comparable energy density at a scale factor

$$\frac{a_\star}{a_i} \equiv \left(\frac{3\phi_{0,i}}{4M}\right)^{-2} \ln\left(\frac{m_\phi^2}{m_{\gamma'}^2}\frac{\phi_{0,i}^2}{m_\phi^2}\right)^2. \tag{31}$$

For $\phi_{0,i}/M = 1$ and $m_{\gamma'} = 10^{-18}$ eV (choosing $\phi_{0,i}$ to match the relic abundance of dark matter—see Sec. IV), $a_\star/a_i \approx 7.1 \times 10^4$, decreasing only by a factor of 2.3 for $m_{\gamma'} = 10^{-6}$ eV.

The above results apply only while modes remain in the small-amplitude resonance band. While the instability extends to arbitrarily small amplitudes when the vector's mass is precisely half the dilaton's, resonance will terminate early if the mass ratio is not so precisely tuned. Concretely, the $n = 1$ band must have nonzero width in k at sufficiently small $|q| \propto \phi_0/M$. Requiring that low-momentum modes do not leave the instability region by the time resonance becomes efficient—namely, that Eq. (24) remains satisfied for some range of k until the Universe expands by $a_\star/a$—we arrive at

$$|\delta| < \frac{3\phi_{0,i}}{16M(a_\star/a_i)^{3/2}} \lesssim 10^{-7}\left(\frac{\phi_{0,i}}{2M}\right)^4 \tag{32}$$

for masses $m_{\gamma'} \sim 10^{-18}$ eV.

While other narrow-band resonances exist (e.g., if $m_{\gamma'}$ is slightly smaller than $2m_\phi$ or for other mass ratios $m_{\gamma'} = nm_\phi/2$), they are centered at nonzero k (in contrast to the low-momentum $n = 1$ band) and shrink in width as the dilaton's amplitude decays. The redshifting of momenta in FLRW spacetime therefore prevents any mode from growing large enough to deplete the dilaton background of its energy density in such cases.

IV. DARK MATTER ABUNDANCE

We now determine the parameter space for which dark photons make up all of the dark matter. The dark matter must have been produced sufficiently long before scales observable in the CMB become dynamical, so production takes place deep in the radiation-dominated era. The dilaton begins oscillating when $H \approx m_\phi$; at this stage, it contains a negligible fraction of the total energy of the Universe (else the matter-dominated era begins too early). Once the dilaton transfers a substantial fraction of its energy to the dark photons, the subsequent evolution is nonlinear—in particular, the excited vector field modes rapidly backreact on the dilaton background. We assume for simplicity that most of the dilaton energy is transferred into the dark photons[3] so that the dilaton makes a negligible contribution to the dark matter abundance. If the dark photons are nonrelativistic when produced,[4] their abundance today is simply

$$\frac{\Omega_{\gamma'}h^2}{0.12} \approx \left(\frac{m_{\gamma'}}{10^{-17}\text{ eV}}\right)^{1/2}\left(\frac{\phi_{0,i}}{10^{16}\text{ GeV}}\right)^2, \tag{33}$$

taking $g_\star = 10.75$ effective number of relativistic degrees of freedom in the plasma at the time of production.

CMB observations place two further constraints on parameter space. First, ensuring that the dark matter was produced before scales observed in the CMB reenter the horizon imposes a lower limit on the vector mass in the $m_{\gamma'} = m_\phi/2$, small-amplitude regime because the Universe expands by a substantial amount before resonance becomes efficient. Namely, using conservation of entropy and Eq. (31), the redshift of production $z_\star = a_0/a_\star - 1$ satisfies

$$\frac{z_\star + 1}{1.9 \times 10^5} = \left(\frac{\phi_{0,i}}{M}\right)^2\left(\frac{m_{\gamma'}}{10^{-17}\text{ eV}}\right)^{1/2} \tag{34}$$

(dropping additional logarithmic dependence on m_ϕ and $\phi_{0,i}$). Since the redshift of matter-radiation equality is $\approx$3400 [51], for masses $m_{\gamma'} \lesssim 10^{-17}$ eV, dark photons are not produced early enough if $\phi_{0,i}/M < 1$. However, lighter masses can be accommodated by a modest increase in amplitude $\phi_{0,i}/M \propto m_{\gamma'}^{-1/4}$.

Second, in this scenario, the vacuum expectation value of the dilaton arises from quantum fluctuations during inflation. The value of $\phi_{0,i}$ varies across causally disconnected Hubble patches and generates an isocurvature perturbation after the decay into dark photons. The power of the isocurvature perturbation from inflation is $\mathcal{P}_S = H_I^2/(\pi\phi_{0,i})^2$, where H_I is the Hubble scale during inflation. Assuming $\Omega_{\gamma'} = \Omega_{\rm DM}$,

[3]Classical lattice simulations demonstrate efficient depletion of an oscillating dilaton into massless dark photons [12,14,41,42] in the strong coupling regime. Furthermore, in similar models with an axial coupling rather than a dilatonic one, most of the energy is transferred to the dark photons, regardless of whether they are massless [13,43–50] or not [15]. Determining whether the same conclusion holds in the small-amplitude regime would require dedicated numerical simulations.

[4]As discussed previously, in the small-amplitude regime with $m_{\gamma'} = m_\phi/2$, the dark photons are necessarily nonrelativistic at production, since $a_\star/a_i \gg 1$ via Eq. (31). In the broad resonance regime (for any $m_{\gamma'} \lesssim m_\phi$ and sufficiently large $\phi_{0,i}/M > 1$), the dark photons are instead mildly relativistic at production, leading to a corresponding dilution in their abundance since they redshift more rapidly than matter until they become nonrelativistic. In this case, the predictions should be analogous to dark photons resonantly produced by axions [15].

CMB constraints on isocurvature perturbations [52] bound the Hubble scale during inflation to be below

$$H_I < 3 \times 10^{11}\ \mathrm{GeV}\left(\frac{m_{\gamma'}}{10^{-17}\ \mathrm{eV}}\right)^{-1/4}. \tag{35}$$

V. DISCUSSION AND CONCLUSIONS

We have demonstrated that a massive vector field kinetically coupled to an oscillating scalar field exhibits a novel nonlinear decay channel. Namely, in addition to a strong-coupling regime reminiscent of axion–dark-photon models [15,33], an oscillating dilaton twice as heavy as its coupled dark photon induces substantial vector production even for small oscillation amplitudes. This effect allows for the efficient production of dark photon dark matter without invoking large couplings, naturally giving rise to dark photon dark matter over a wide range of masses. Efficient parametric resonance in the small-coupling regime requires a finely tuned mass ratio $m_{\gamma'}/m_\phi = 1/2$—as severe as one part in 10^7 for order-unity couplings—barring a UV model that gives rise to both the dark photon and dilaton's masses and explains the coincidence.

In Sec. IV, we showed that requiring consistency with the CMB jointly constrains the vector mass and coupling strength, but only modestly large couplings are required to achieve ultralight masses $\sim 10^{-20}$ to 10^{-18} eV. To go beyond these estimates (e.g., to characterize the relic abundance of dark photons and dilatons as a function of the particle masses and initial field amplitudes and to compute the resulting spectra of dark photons) requires $3+1$D numerical simulations. Preliminary simulations confirm the numerical and parametric estimates of Secs. III B and IV, but we leave a more thorough investigation of these questions to future work.

The rapid growth of vector modes and nonlinear dynamics at the end of the production phase would source a gravitational wave background, providing a possible probe of the model. Though a quantitative prediction would again require dedicated numerical study, the signals are likely to resemble those from dark photons resonantly produced by a rolling axion [49,50,53–55]. However, the signal amplitude is unlikely to be promisingly large. Stochastic backgrounds are parametrically suppressed by both the fraction of Universe's net energy density contained by the source and the gravitational-wave wavelength relative to the horizon size at production [56]. In this scenario, the vector and dilaton are massive relics whose abundance is $\propto a_\star/a_{\mathrm{eq}}$, i.e., the ratio of the scale factors at production and matter-radiation equality. One might then expect the long delay from oscillation (a_i) to production ($a_\star$) to enhance the resulting signals, but gravitational wave emission occurs at fixed comoving scales $\sim m_\phi$ that are $a_\star/a_i$ times farther inside the horizon at production. These two effects turn out to cancel each other, and even highly efficient gravitational wave production is unlikely to exceed present-day abundances of $\Omega_{\mathrm{GW},0} \sim 10^{-15}$ (see, e.g., Ref. [57]).

Here, we specifically invoke a dilatonic coupling to achieve dark matter predominantly comprising dark photons. In principle, the dilaton could instead be the dark matter and simply happen to have such a coupling with parameter values that fail to achieve efficient conversion to dark photons before the CMB forms. For the same reason that resonance could become efficient at sufficiently late times in the radiation era even for small couplings [as discussed after Eq. (26)], in this alternative scenario, substantial dark photon production will *never* occur: As the Universe transitions to matter domination, the Hubble rate instead decays as $a^{-3/2}$ just like the dilaton, and the growth rate per Hubble time asymptotes to a constant. In other words, if the dilaton has not efficiently produced dark photons by the time the CMB forms, then it never will. (The marginal regime—resonance becoming efficient as CMB modes enter the horizon—would likely be incompatible with the cold, collisionless dark matter required by CMB observations.)[5]

While we have not assumed any particular origin for the mass of the dark photon, in the case where the mass arises from the Higgs mechanism, the production of vortices challenges the viability of dark photon dark matter [58]. Moreover, as noted by [15,59,60], Stueckelberg masses are restricted to $m_{\gamma'} \gtrsim$ meV in string theory, implying that smaller masses must arise from the Higgs mechanism. To our knowledge, all proposed production mechanisms for light dark photon dark matter are afflicted by vortex formation constraints. However, it is possible that the small-amplitude regime we point out could evade such issues: The long delay between dilaton oscillations and dark photon production could ensure the vector's energy density never exceeds the critical value for vortex formation. We defer a full exploration of the parameter dependence of vortex formation constraints, along with the phenomenology of kinetic mixing with the Standard Model photon and subsequent plasma effects, to future work.[6]

Throughout this work, we assumed that the dark photon mass is ϕ independent. This dependence, like the form of the kinetic coupling $W(\phi)$, is ultimately determined by the UV physics. Providing a UV completion of the theory is beyond the scope of this work, but it is conceivable that both the kinetic and mass terms attain a ϕ dependence, coming from, e.g., radiative corrections. [In fact, the small-amplitude resonance is present if the coupling function $W(\phi)$ multiplies the mass term rather than the kinetic term of the vector since the pertinent terms in the equation of

[5]We thank an anonymous referee for pointing out this interesting feature of the model.

[6]A kinetic mixing term would nominally induce resonant production of Standard Model photons (depending on, e.g., its plasma mass) as well, but the kinetic mixing parameter must be (much) smaller than 10^{-6} to 10^{-10} (depending on the dark photon mass) [61], greatly suppressing this effect.

motion have the same form.] Such interactions, as well as dark photon self-interactions, could have consequences for the efficiency of dark photon production and the viable parameter space for dark photon dark matter. We leave the investigation of such effects for future work.

ACKNOWLEDGMENTS

We thank Mustafa Amin and David Cyncynates for comments on a draft of this paper, and Z. J. W. also thanks David Cyncynates for extensive discussions about dark photons. P. A. thanks the Center for Particle Cosmology at the University of Pennsylvania for hospitality while this work was being completed. The work of P. A. and K. L. is supported in part by the United States Department of Energy, DE-SC0015655. Z. J. W. is supported by the Department of Physics and the College of Arts and Sciences at the University of Washington. This work made use of the PYTHON packages NumPy [62], SciPy [63], Matplotlib [64], SymPy [65], and CMasher [66].

[1] W. Hu, R. Barkana, and A. Gruzinov, Cold and Fuzzy Dark Matter, Phys. Rev. Lett. **85**, 1158 (2000).
[2] H.-Y. Schive, T. Chiueh, and T. Broadhurst, Cosmic structure as the quantum interference of a coherent dark wave, Nat. Phys. **10**, 496 (2014).
[3] L. Hui, J. P. Ostriker, S. Tremaine, and E. Witten, Ultralight scalars as cosmological dark matter, Phys. Rev. D **95**, 043541 (2017).
[4] L. Hui, Wave dark matter, Annu. Rev. Astron. Astrophys. **59**, 247 (2021).
[5] P. Adshead and K. D. Lozanov, Self-gravitating vector dark matter, Phys. Rev. D **103**, 103501 (2021).
[6] B. Salehian, H.-Y. Zhang, M. A. Amin, D. I. Kaiser, and M. H. Namjoo, Beyond Schrödinger-Poisson: Nonrelativistic effective field theory for scalar dark matter, J. High Energy Phys. 09 (2021) 050.
[7] M. Jain and M. A. Amin, Polarized solitons in higher-spin wave dark matter, Phys. Rev. D **105**, 056019 (2022).
[8] M. A. Amin, M. Jain, R. Karur, and P. Mocz, Small-scale structure in vector dark matter, J. Cosmol. Astropart. Phys. 08 (2022) 014.
[9] H.-Y. Zhang, M. Jain, and M. A. Amin, Polarized vector oscillons, Phys. Rev. D **105**, 096037 (2022).
[10] M. Jain, Soliton stars in Yang-Mills-Higgs theories, Phys. Rev. D **106**, 085011 (2022).
[11] P. W. Graham, J. Mardon, and S. Rajendran, Vector dark matter from inflationary fluctuations, Phys. Rev. D **93**, 103520 (2016).
[12] J. T. Deskins, J. T. Giblin, and R. R. Caldwell, Gauge field preheating at the end of inflation, Phys. Rev. D **88**, 063530 (2013).
[13] P. Adshead, J. T. Giblin, T. R. Scully, and E. I. Sfakianakis, Gauge-preheating and the end of axion inflation, J. Cosmol. Astropart. Phys. 12 (2015) 034.
[14] P. Adshead, J. T. Giblin, and Z. J. Weiner, Gravitational waves from gauge preheating, Phys. Rev. D **98**, 043525 (2018).
[15] P. Agrawal, N. Kitajima, M. Reece, T. Sekiguchi, and F. Takahashi, Relic abundance of dark photon dark matter, Phys. Lett. B **801**, 135136 (2020).
[16] M. Gorghetto, E. Hardy, J. March-Russell, N. Song, and S. M. West, Dark photon stars: Formation and role as dark matter substructure, J. Cosmol. Astropart. Phys. 08 (2022) 018.
[17] N. Dalal and A. Kravtsov, Excluding fuzzy dark matter with sizes and stellar kinematics of ultrafaint dwarf galaxies, Phys. Rev. D **106**, 063517 (2022).
[18] M. A. Amin and M. Mirbabayi, A lower bound on dark matter mass, arXiv:2211.09775.
[19] A. Arvanitaki, S. Dimopoulos, S. Dubovsky, N. Kaloper, and J. March-Russell, String axiverse, Phys. Rev. D **81**, 123530 (2010).
[20] A. Arvanitaki and S. Dubovsky, Exploring the string axiverse with precision black hole physics, Phys. Rev. D **83**, 044026 (2011).
[21] A. Arvanitaki, M. Baryakhtar, S. Dimopoulos, S. Dubovsky, and R. Lasenby, Black hole mergers and the QCD axion at Advanced LIGO, Phys. Rev. D **95**, 043001 (2017).
[22] M. Baryakhtar, M. Galanis, R. Lasenby, and O. Simon, Black hole superradiance of self-interacting scalar fields, Phys. Rev. D **103**, 095019 (2021).
[23] M. Baryakhtar, R. Lasenby, and M. Teo, Black hole superradiance signatures of ultralight vectors, Phys. Rev. D **96**, 035019 (2017).
[24] V. Cardoso, O. J. C. Dias, G. S. Hartnett, M. Middleton, P. Pani, and J. E. Santos, Constraining the mass of dark photons and axionlike particles through black-hole superradiance, J. Cosmol. Astropart. Phys. 03 (2018) 043.
[25] A. E. Nelson and J. Scholtz, Dark light, dark matter and the misalignment mechanism, Phys. Rev. D **84**, 103501 (2011).
[26] P. Arias, D. Cadamuro, M. Goodsell, J. Jaeckel, J. Redondo, and A. Ringwald, WISPy cold dark matter, J. Cosmol. Astropart. Phys. 06 (2012) 013.
[27] G. Alonso-Álvarez, T. Hugle, and J. Jaeckel, Misalignment & Co.: (Pseudo-)scalar and vector dark matter with curvature couplings, J. Cosmol. Astropart. Phys. 02 (2020) 014.
[28] F. Elahi and S. Khatibi, Light non-Abelian vector dark matter produced through vector misalignment, arXiv:2204.04012.
[29] Y. Ema, K. Nakayama, and Y. Tang, Production of purely gravitational dark matter: The case of fermion and vector boson, J. High Energy Phys. 07 (2019) 060.
[30] E. W. Kolb and A. J. Long, Completely dark photons from gravitational particle production during the inflationary era, J. High Energy Phys. 03 (2021) 283.

[31] A. Ahmed, B. Grzadkowski, and A. Socha, Gravitational production of vector dark matter, J. High Energy Phys. 08 (2020) 059.
[32] J. A. Dror, K. Harigaya, and V. Narayan, Parametric resonance production of ultralight vector dark matter, Phys. Rev. D **99**, 035036 (2019).
[33] R. T. Co, A. Pierce, Z. Zhang, and Y. Zhao, Dark photon dark matter produced by axion oscillations, Phys. Rev. D **99**, 075002 (2019).
[34] Y. Nakai, R. Namba, and Z. Wang, Light dark photon dark matter from inflation, J. High Energy Phys. 12 (2020) 170.
[35] K. Nakayama, Constraint on vector coherent oscillation dark matter with kinetic function, J. Cosmol. Astropart. Phys. 08 (2020) 033.
[36] Y. Nakai, R. Namba, and I. Obata, Peaky production of light dark photon dark matter, arXiv:2212.11516.
[37] W. Magnus and S. Winkler, *Hill's Equation*, Dover Books on Mathematics Series (Dover Publications, New York, 2004).
[38] M. A. Amin, M. P. Hertzberg, D. I. Kaiser, and J. Karouby, Nonperturbative dynamics of reheating after inflation: A review, Int. J. Mod. Phys. D **24**, 1530003 (2014).
[39] T. S. Bunch and P. C. W. Davies, Quantum field theory in de Sitter space: Renormalization by point splitting, Proc. R. Soc. A **360**, 117 (1978).
[40] N. D. Birrell and P. C. W. Davies, *Quantum Fields in Curved Space*, Cambridge Monographs on Mathematical Physics (Cambridge University Press, Cambridge, UK, 1984).
[41] J. T. Giblin, G. Kane, E. Nesbit, S. Watson, and Y. Zhao, Was the universe actually radiation dominated prior to nucleosynthesis?, Phys. Rev. D **96**, 043525 (2017).
[42] P. Adshead, J. T. Giblin, and Z. J. Weiner, Non-Abelian gauge preheating, Phys. Rev. D **96**, 123512 (2017).
[43] P. Adshead, J. T. Giblin, T. R. Scully, and E. I. Sfakianakis, Magnetogenesis from axion inflation, J. Cosmol. Astropart. Phys. 10 (2016) 039.
[44] D. G. Figueroa and M. Shaposhnikov, Lattice implementation of Abelian gauge theories with Chern–Simons number and an axion field, Nucl. Phys. **B926**, 544 (2018).
[45] J. R. C. Cuissa and D. G. Figueroa, Lattice formulation of axion inflation. Application to preheating, J. Cosmol. Astropart. Phys. 06 (2019) 002.
[46] P. Adshead, J. T. Giblin, M. Pieroni, and Z. J. Weiner, Constraining Axion Inflation with Gravitational Waves across 29 Decades in Frequency, Phys. Rev. Lett. **124**, 171301 (2020).
[47] P. Adshead, J. T. Giblin, M. Pieroni, and Z. J. Weiner, Constraining axion inflation with gravitational waves from preheating, Phys. Rev. D **101**, 083534 (2020).
[48] N. Kitajima, J. Soda, and Y. Urakawa, Nano-Hz Gravitational-Wave Signature from Axion Dark Matter, Phys. Rev. Lett. **126**, 121301 (2021).
[49] W. Ratzinger, P. Schwaller, and B. A. Stefanek, Gravitational waves from an axion-dark photon system: A lattice study, SciPost Phys. **11**, 001 (2021).
[50] Z. J. Weiner, P. Adshead, and J. T. Giblin, Constraining early dark energy with gravitational waves before recombination, Phys. Rev. D **103**, L021301 (2021).
[51] N. Aghanim *et al.* (Planck Collaboration), Planck 2018 results. VI. Cosmological parameters, Astron. Astrophys. **641**, A6 (2020); **652**, C4(E) (2021).
[52] Y. Akrami *et al.* (Planck Collaboration), Planck 2018 results. X. Constraints on inflation, Astron. Astrophys. **641**, A10 (2020).
[53] C. S. Machado, W. Ratzinger, P. Schwaller, and B. A. Stefanek, Audible axions, J. High Energy Phys. 01 (2019) 053.
[54] C. S. Machado, W. Ratzinger, P. Schwaller, and B. A. Stefanek, Gravitational wave probes of axionlike particles, Phys. Rev. D **102**, 075033 (2020).
[55] B. Salehian, M. A. Gorji, S. Mukohyama, and H. Firouzjahi, Analytic study of dark photon and gravitational wave production from axion, J. High Energy Phys. 05 (2021) 043.
[56] J. T. Giblin and E. Thrane, Estimates of maximum energy density of cosmological gravitational-wave backgrounds, Phys. Rev. D **90**, 107502 (2014).
[57] D. Cyncynates, O. Simon, J. O. Thompson, and Z. J. Weiner, Nonperturbative structure in coupled axion sectors and implications for direct detection, Phys. Rev. D **106**, 083503 (2022).
[58] W. E. East and J. Huang, Dark photon vortex formation and dynamics, J. High Energy Phys. 12 (2022) 089.
[59] M. Goodsell, J. Jaeckel, J. Redondo, and A. Ringwald, Naturally light hidden photons in LARGE volume string compactifications, J. High Energy Phys. 11 (2009) 027.
[60] M. Reece, Photon masses in the landscape and the Swampland, J. High Energy Phys. 07 (2019) 181,
[61] A. Caputo, A. J. Millar, C. A. J. O'Hare, and E. Vitagliano, Dark photon limits: A handbook, Phys. Rev. D **104**, 095029 (2021).
[62] C. R. Harris *et al.*, Array programming with NumPy, Nature (London) **585**, 357 (2020).
[63] P. Virtanen *et al.*, SciPy 1.0–fundamental algorithms for scientific computing in PYTHON, Nat. Methods **17**, 261 (2020).
[64] J. D. Hunter, Matplotlib: A 2D graphics environment, Comput. Sci. Eng. **9**, 90 (2007).
[65] A. Meurer *et al.*, SymPy: Symbolic computing in PYTHON, PeerJ Comput. Sci. **3**, e103 (2017).
[66] E. van der Velden, CMasher: Scientific colormaps for making accessible, informative and 'cmashing' plots, J. Open Source Softwaare **5**, 2004 (2020).